Mechanical Stability Analysis of Engineering Structures with Use of the Bifurcation Domain Concept

Antoine Wautier[1(✉)], Anthony Mouyeaux[1], François Nicot[2,3], Richard Wan[4], and Félix Darve[5]

[1] INRAE, Aix Marseille University, UMR RECOVER, Aix-en-Provence, Marseille, France
antoine.wautier@inrae.fr

[2] Université Grenoble Alpes, INRAE, UR ETNA, St-Martin-d'Hères, France

[3] Laboratoire EDYTEM - USMB/CNRS, UMR 5204, Université Savoie Mont Blanc, Le Bourget-du-Lac, France

[4] Civil Engineering Department, University of Calgary, Calgary, AB, Canada

[5] Laboratoire 3SR UMR5521, Université Grenoble Alpes, CNRS, G-INP, Grenoble, France

Abstract. Because of their non-associated plastic behavior, the failure modes of geomaterials are much more diverse than those of materials following associated plasticity. For instance, it is well established that failure can occur before reaching the plastic limit surface and before the vanishing of the determinant of the acoustic tensor. This is well illustrated by the static liquefaction of loose sand subjected to undrained triaxial tests in the lab or by the recent failure of Brumadinho dam in 2019. In the wake of the pioneering work of Hill [4], the second-order work criterion, as proposed by Nicot et al. [11], Wan et al. [18], has been shown to be the most general criterion to anticipate failure for non-associated materials. This criterion defines a bifurcation domain corresponding to a set of states for which there exists a potential for failure if (i) the material is subjected to an incremental load leading to the vanishing of the second-order work, (ii) the mode of control allows for an inertial transition through a sudden burst of kinetic energy. In this work, it is proposed to extend the concept of bifurcation domain from the material point scale to the engineering structure scale. In this respect, an earth dam is modeled using the finite element software Cast3M [3]. By virtue of directional analyses carried out both numerically and analytically at different location points in the dam body, the set of material points that belongs to the bifurcation domain is identified. This enables us to map the spatial domain of the dam where conditional failure may occur. This map can be used to anticipate unsafe changes in loading conditions on the dam boundaries. Such a contribution proposes a modern and innovative view of failure in geomaterials at the engineering scale, in particular with respect to the risk of liquefaction.

Keywords: Mechanical stability · Second-order work criterion · Engineering scale · Liquefaction

E. Pasternak and A. Dyskin (Eds.): IWBDG 2022, 2023.
https://doi.org/10.1007/978-3-031-22213-9_1

1 Introduction

A correct design of engineering structures relies on an accurate prediction of failure modes. Historically, the mechanical stability analysis of earth dikes or dams has been assessed thanks to Limit Equilibrium Methods (LEM) [2, 15, 16]. Such methods postulate the existence of a failure surface with a given geometry (usually circular) and the equilibrium of the expected sliding mass is solved by dividing it into slices in contact. Repeating the procedure for several failure surfaces enables us to assess the stability of the structure. In this approach, the failure mechanism is postulated a priori, which leads to the definition of an upper bound for mechanical stability. Since there could exist other failure mechanisms not accounted for, safety margins are considered with the use of a large safety factor (the ratio between resistive forces over the maximal resistive forces allowed by the sliding criterion). LEM methods are still frequently used in engineering approaches, because of their simplicity and even if they generally lead to overdesign.

With the increase in computer power, more refined methods were proposed based on the use of Finite Element Modeling (FEM). Based on the knowledge of the material constitutive behaviors and the designed geometry, stress and strain fields can be computed. Zones in which the mechanical state is close to the failure limit are then identified, as well as potential failure surfaces. As long as the numerical computation converge, the static equilibrium of the structure is obtained. In this sense, FEM provides a lower bound for mechanical stability. However, to account for uncertainties in determining material properties, a safety factor is also used. In FEM framework, it can be defined with the use of the shear strength reduction technique [21]. This technique consists in decreasing the shear resistance of the soil until failure occurs, which is often detected in practice from a lack in numerical convergence.

In both cases, the standard engineering methods used to assess the mechanical stability of earth dikes or dams relate the current stress state to the plastic ultimate state that the soil can bear without considering any perturbation. However, geomaterials are known to exhibit a non-associated plastic behavior. As a result, their failure modes are much more diverse than those of materials following associated plasticity. They can fail before reaching the plastic limit surface through the formation of shear bands for instance, or through static liquefaction. The formation of shear bands is well detected by the vanishing of the determinant of the acoustic tensor [8, 14] but not the static liquefaction (frequently observed for loose sand subjected to undrained triaxial tests) which requires the use of the second-order work criterion [4, 11, 18, 19]. The second-order work criterion corresponds to the loss of positive definitiveness of the elasto-plastic matrix, i.e. when the determinant of the symmetric part of this matrix is negative. For associated plasticity, the elasto-plastic matrix is symmetric and material bifurcations appear therefore on the plastic limit surface. But for non-associated plasticity, the vanishing of the second-order work occurs strictly before the plastic limit conditions is fulfilled and before the vanishing of the accoustic tensor [1, 18]. Under the assumptions of small strains and negligible geometrical effects, the second-order work criterion reads:

$$\exists(\mathrm{d}\boldsymbol{\sigma}, \mathrm{d}\boldsymbol{\varepsilon}) \text{ linked by the constitutive behavior such that } W_2 = \mathrm{d}\boldsymbol{\sigma} : \mathrm{d}\boldsymbol{\varepsilon} < 0 \quad (1)$$

The second-order work criterion defines the concept of bifurcation domain at the material point scale which corresponds to the set of states (defined by states variables) for which conditional failure is expected [17, 18]. For such states, a proper loading direction and a proper mode of control will trigger material failure in the form of an inertial transition from a quasi-static to a dynamic regime [19]. Such potential for failure is assessed at the material point scale thanks to the use of directional analyses [19], which consists in applying any possible stress or strain perturbation form a reference state, recording the material response and evaluating the sign of the corresponding second order work.

At the engineering structure scale, the vanishing of the second-order work was used so far only along a given loading path in order to anticipate the failure of the structure [5, 7, 10, 13, 20]. Such approaches have proved to be relevant to detecting the onset of instabilities when the engineering structure is subjected to a monotonic change of its boundary conditions, but such approaches fails to predict whether there exists any critical incremental perturbations detrimental to safety for a structure at equilibrium initially. To the best of our knowledge, only the work of Prunier, Laouafa et al. [6, 12] provided some clues to answer this question at the scale of an engineering structure, by observing the vanishing of the determinant of the global stiffness matrix that relates to unknown degrees of freedom of a FEM problem. Such an approach is however computationally demanding because the size of the matrix is huge.

The present work intends to apply the concept of bifurcation domain at the engineering structure scale. FEM simulations are conducted for a dam made of a non-associated Drucker-Prager elasto-plastic material. For each point of the dam, strain control directional analyses are conducted from an analytical point of view to detect which points of the dam are in the bifurcation domain from a material scale viewpoint. By analyzing the directions of the instability cone thus detected, the existence of potential internal failure surfaces are estimated. The present study intends to generalize the use of second-order work at the scale of an engineering structure, and the notion of conditional stability in mechanical stability analyses. In the context of dam safety, we hope that our methodology may be used to better anticipate failure through static liquefaction as illustrated by the Brumadinho dam failure in 2019 in Brazil.

2 Dam Modeling with FEM

In this study, a simple trapezoidal dam is modeled in plane strain conditions with the finite element software Cast3M [3]. The dam body and the foundation are both assumed to behave as a standard non-associated elasto-plastic material following Drucker-Prager criterion. The constitutive behavior is summarized as

$$\begin{cases} \text{Elasticity (Hooke law) :} & \boldsymbol{\sigma} = \lambda \mathrm{Tr}(\boldsymbol{\varepsilon^e})\mathbf{1} + 2\mu\boldsymbol{\varepsilon^e} \\ \text{Strain decomposition:} & \boldsymbol{\varepsilon} = \boldsymbol{\varepsilon^e} + \boldsymbol{\varepsilon^p} \\ \text{Drucker-Prager yield surface:} & f(\boldsymbol{\sigma}) = \alpha \mathrm{Tr}(\boldsymbol{\sigma}) + \sigma_{eq} < K \\ \text{Drucker-Prager plastic potential:} & g(\boldsymbol{\sigma}) = \beta \mathrm{Tr}(\boldsymbol{\sigma}) + \sigma_{eq} \\ \text{Non-associated flow rule:} & \dot{\boldsymbol{\varepsilon}}^{\boldsymbol{p}} = \dot{\eta}\frac{\partial g}{\partial \boldsymbol{\sigma}} = \dot{\eta}\left(\beta\mathbf{1} + \frac{3}{2}\frac{\boldsymbol{\sigma}}{\sigma_{eq}}\right),\ \dot{\eta} \geq 0 \\ \text{Hardening (not activated) :} & \dot{K} = H\dot{\varepsilon}^p_{eq},\ K \in [K_0, K_{max}] \end{cases} \quad (2)$$

In the above equations, the invariants σ_{eq} and ε^p_{eq} are expressed as $\sigma_{eq} = \sqrt{\frac{3}{2}\boldsymbol{s} : \boldsymbol{s}}$ with $\boldsymbol{s} = \boldsymbol{\sigma} - \frac{1}{3}\mathrm{Tr}(\boldsymbol{\sigma})\mathbf{1}$ the deviatoric stress tensor, and $\varepsilon^p_{eq} = \sqrt{\frac{2}{3}\boldsymbol{\varepsilon^p_{dev}} : \boldsymbol{\varepsilon^p_{dev}}}$ with $\boldsymbol{\varepsilon^p_{dev}} = \boldsymbol{\varepsilon^p} -$

$\frac{1}{3}\mathrm{Tr}(\boldsymbol{\varepsilon}^{\boldsymbol{p}})\mathbf{1}$ the deviatoric part of the plastic strain. In all this study, continuum mechanics sign convention is used with positive traction and extension. Note that hardening can be accounted for if $H > 0$.

In plane strain conditions, the plastic coefficients α, β and K can be expressed in terms of friction angle φ, cohesion c' and dilatancy angle ψ (see for instance [9]), while the elastic Lamé coefficients relates to Young's modulus E and Poisson's ratio ν as:

$$\left\{\begin{array}{ll} \lambda &= \frac{E\nu}{(1+\nu)(1-2\nu)} \\ \mu &= \frac{E}{2(1+\nu)} \end{array}\right. , \quad \left\{\begin{array}{ll} \alpha &= \frac{\sqrt{3}\tan\varphi}{\sqrt{9+12\tan^2\varphi}} \\ \beta &= \frac{\sqrt{3}\tan\psi}{\sqrt{9+12\tan^2\psi}} \\ K_0 &= \frac{3\sqrt{3}c'}{\sqrt{9+12\tan^2\varphi}} \end{array}\right. . \tag{3}$$

The material parameters and the geometrical characteristics of the dam are summarized in Table 1. The dam has a drainage system located on the interface with the foundation and starting 10 m downstream from the middle of the crest.

The static equilibrium of the dam is computed with a simplified two steps procedure:

1. In the first step, gravity is progressively increased while the water reservoir remains empty. The dam geometry is set once for all and the construction of a real dam in lifts is not accounted for. Thus, this step corresponds to an approximate modeling of the dam construction.
2. Then, a pore water pressure field is applied by gradually increasing the pore water pressure from zero to the values corresponding to a column of 7 m in the dam reservoir. This step corresponds roughly to the filling of the dam reservoir. The water pressure field is obtained from a separate hydraulic simulation performed in Cast3M with an horizontal hydraulic permeability of 10^{-6} m/s in the dam body and in the foundation and of 10^{-3} m/s in the drainage system. In both cases, anisotropic permeability is considered with the vertical permeability being ten times larger. The pore water pressure field is applied in the form of external forces on the mesh elements according to local pressure gradients.

Once the mechanical equilibrium is achieved, the stress and strain fields are extracted to be analyzed from a material point scale with respect to the concept of bifurcation domain.

3 Material Scale Stability Analysis

If we limit our analyses to divergence instabilities, it is well established that the most general criterion to study these bifurcations is the so-called *second-order work criterion* (1) as introduced by Hill [4] and reviewed extensively in [18]. Based on this definition, the mechanical stability of a material is assessed thanks to directional analyses. For instance, this can be performed in the strain space, by imposing $\mathrm{d}\boldsymbol{\varepsilon}$ and recording $\mathrm{d}\boldsymbol{\sigma}$ according to the constitutive behavior. In the most general case, $\mathrm{d}\boldsymbol{\varepsilon}$ resides in a space of six dimensions. However, by considering the principal strain directions, the directional

Table 1. Material parameters and the geometrical characteristics of the dam.

	E (MPa)	ν	φ (°)	ψ (°)	c' (kPa)	H (kPa)	ρ (kg m^{-3})	Height (m)	Crest width (m)	Slopes
Dam	45	0.35	25	12	5	0	2150	10	6	1.25 H/1 V
Foundation	50	0.35	25	12	5	0	2150	–	–	–

analysis can be restricted to the diagonal $\mathrm{d}\boldsymbol{\varepsilon}$ with only three independent components. By use of the spherical coordinates, $\mathrm{d}\boldsymbol{\varepsilon}$ is imposed as:

$$\begin{cases} \mathrm{d}\varepsilon_I &= \mathrm{d}\varepsilon \cos\phi \sin\theta \\ \mathrm{d}\varepsilon_{II} &= \mathrm{d}\varepsilon \sin\phi \sin\theta \\ \mathrm{d}\varepsilon_{III} &= \mathrm{d}\varepsilon \cos\theta \end{cases} \tag{4}$$

with $\theta \in [0, \pi]$ and $\phi \in [0, 2\pi]$. θ and ϕ correspond to the *direction* of the incremental strain perturbation in the principal strain space.

For the constitutive behavior summarized in Eq. (2), an analytical expression can be derived for W_2. The expression depends on whether plasticity is activated, the plasticity activation condition being $f(\boldsymbol{\sigma} + \mathrm{d}\boldsymbol{\sigma}^e) > K$ where $\mathrm{d}\boldsymbol{\sigma}^e = \lambda \mathrm{Tr}(\mathrm{d}\boldsymbol{\varepsilon})\mathbf{1} + 2\mu \mathrm{d}\boldsymbol{\varepsilon}$.

– In the elastic case, $f(\boldsymbol{\sigma} + \mathrm{d}\boldsymbol{\sigma}^e) < K$, and the second-order work reads:

$$W_2^e = K_{comp}\mathrm{Tr}^2(\mathrm{d}\boldsymbol{\varepsilon}) + 2\mu||\mathrm{d}\boldsymbol{\varepsilon}_{dev}||^2 \tag{5}$$

– In the plastic case, $f(\boldsymbol{\sigma} + \mathrm{d}\boldsymbol{\sigma}^e) > K$, and the second-order work reads:

$$W_2^p = W_2^e - \frac{\left[\frac{f(\boldsymbol{\sigma})-K}{3} + \alpha K_{comp}\mathrm{Tr}(\mathrm{d}\boldsymbol{\varepsilon}) + \mu\frac{\boldsymbol{s}:\mathrm{d}\boldsymbol{\varepsilon}_{\boldsymbol{dev}}}{\sigma_{eq}}\right]\left[\beta K_{comp}\mathrm{Tr}(\mathrm{d}\boldsymbol{\varepsilon}) + \mu\frac{\boldsymbol{s}:\mathrm{d}\boldsymbol{\varepsilon}_{\boldsymbol{dev}}}{\sigma_{eq}}\right]}{\alpha\beta K_{comp} + \frac{\mu}{3} + \frac{H}{9}\frac{\boldsymbol{s}:\mathrm{d}\boldsymbol{\varepsilon}^{\boldsymbol{p}}_{\boldsymbol{dev}}}{\sigma_{eq}\varepsilon^p_{eq}}} \tag{6}$$

In the above equations, $K_{comp} = \lambda + 2\mu/3$ is the compressibility modulus, $\mathrm{d}\boldsymbol{\varepsilon}_{dev}$ and $\boldsymbol{s}$ the deviatoric parts of the incremental strain and the stress tensors respectively.

Note that, plasticity needs to be activated in order to observe the vanishing of the second-order work in (6) as $W_2^e \geq 0$. In that case, it is interesting to underline that hardening ($H > 0$) will limit the possibility to observe the vanishing of the second-order work in (6). If the initial state is on the plastic yield surface ($f(\boldsymbol{\sigma}) = K$), Eq. (6) simplifies a little. And for the case of associated plasticity ($\alpha = \beta$) with no hardening ($H = 0$), the use of Cauchy-Schwarz inequality shows that W_2 is always greater or equal to zero[1].

Based on the analytical expression given in Eqs. (5) and (6), the normalized second-order work $W_2^{norm} = \frac{W_2}{||\mathrm{d}\boldsymbol{\sigma}||||\mathrm{d}\boldsymbol{\varepsilon}||}$ can be plotted with a spherical representation for all the points of the dam body as illustrated in Fig. 1.

In Fig. 1, an elliptical cone of instability is observed in the principal strain space for some points of the dam for incremental loading directions corresponding generally to $\mathrm{d}\varepsilon_I > 0$ (extension), $\mathrm{d}\varepsilon_{II} < 0$ (compression) and $\mathrm{d}\varepsilon_{III} > 0$ (extension). Such results are consistent with the usual instability cone directions observed in the literature [13, 19]. In the case where $\mathrm{d}\varepsilon_I + \mathrm{d}\varepsilon_{II} = 0$ (close to the situation observed in Fig. 1, the cone direction corresponds to pure shear in the plane (e_I, e_{II}) with an extension in the out of plane direction. The elliptical shape of the instability cone has been previously reported in [13] for different constitutive relations.

---

[1] Vanishing requires $\mathrm{d}\boldsymbol{\varepsilon}^{\boldsymbol{p}}_{\boldsymbol{dev}}$ to be positively co-linear to $\boldsymbol{s}$ and $\mathrm{Tr}(\mathrm{d}\boldsymbol{\varepsilon}) = \alpha\sqrt{6}||\mathrm{d}\boldsymbol{\varepsilon}^{\boldsymbol{p}}_{\boldsymbol{dev}}|| > 0$ (increase in volume).

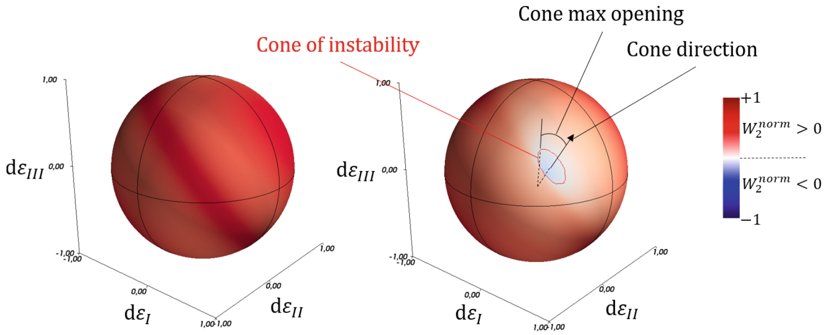

Fig. 1. Spherical representation in the principal strain space of the normalized second-order work for two points of the dam body: out of (left) and in (right) the bifurcation domain. The set of loading directions with $W_2 < 0$ forms an elliptic cone of instability characterized by a mean direction and a maximal opening angle.

4 Bifurcation Domain Definition and Instability Cone Directions

In the previous section, the mechanical stability was assessed from a material scale viewpoint. In order to assess the mechanical stability of an engineering structure according to Eq. (1), there is a need to define the bifurcation domain Ω_{bif} of an engineering structure

$$\begin{aligned} \boldsymbol{x} \in \Omega_{bif} \text{ if and only if } \exists(\mathrm{d}\boldsymbol{\sigma}, \mathrm{d}\boldsymbol{\varepsilon}), \text{ such that} \\ \mathrm{d}\boldsymbol{\sigma} = \boldsymbol{C}(\boldsymbol{\sigma}(\boldsymbol{x})) : \mathrm{d}\boldsymbol{\varepsilon} \text{ and } W_2 = \mathrm{d}\boldsymbol{\sigma} : \mathrm{d}\boldsymbol{\varepsilon} < 0 \end{aligned} \tag{7}$$

where $\boldsymbol{C}(\boldsymbol{\sigma}(\boldsymbol{x}))$ is the tangent constitutive tensor of the material located at point $\boldsymbol{x}$.

For the points located in the bifurcation domain, there exists a set of incremental directions that will lead to material failure (provided that the imposed perturbation on the dam boundaries allows for an increase in kinetic energy). The cone direction (θ_c, ϕ_c) (illustrated in Fig. 1) corresponds to an incremental strain tensor $\mathrm{d}\boldsymbol{\varepsilon}_{cone}$ with principal strain values $(\mathrm{d}\varepsilon_I, \mathrm{d}\varepsilon_{II}, \mathrm{d}\varepsilon_{III})$ expressed according to (4) and principal directions coinciding with the principal strain directions (by definition of the set of incremental strain considered in the directional analysis). Because of the plane strain condition, one principal strain direction is the out of plane direction z. The two other directions lie in the (x, y) plane and depends on the strain field.

A representation of the dam bifurcation domain together with the corresponding strain perturbation leading to the vanishing of the second order work (i.e. the cone directions) is given in Fig. 2.

For the dam considered, the bifurcation domain is quite extensive and looks consistent with the shapes of failure observed in situ. However, one can notice that most of the cone directions have a non negligible off plane component, making them not compatible with plane strain mechanisms. If we restrict the admissible failure mechanisms to plane strain conditions (this correspond to the equatorial plane in Fig. 1), the bifurcation domain is largely reduced as illustrated in Fig. 3. It no longer spans across the dam body.

As a result, we can conclude from these graphs that there exists some plausible mechanisms that can lead to the failure of the dam considered; provided that the plane

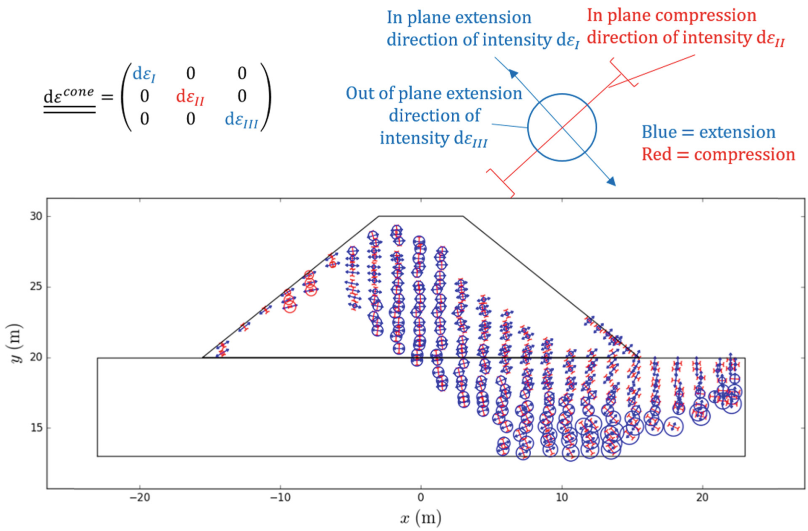

Fig. 2. Bifurcation domain of a dam. For each material point in the bifurcation domain, the cone direction is represented. Such representation corresponds to local deformation mechanisms likely to trigger underlying material instability.

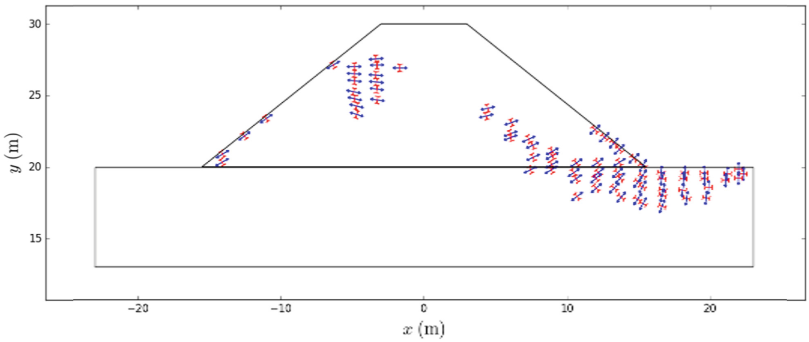

Fig. 3. Bifurcation domain of a dam restricted to plane strain perturbations. For each material point in the bifurcation domain, the plane strain cone direction is represented as in Fig. 2.

strain assumption is lifted. These mechanisms cannot develop fully without allowing an extension of the dam in the out-of-plane direction.

5 Conclusion

In this paper, we have proposed a method to extend the concept of bifurcation domain from the material scale viewpoint to the scale of engineering structures in the form of bifurcation maps. The use of this advanced criterion enables us to think outside the box to detect potential failure modes that are not accounted for in more standard approaches and with more restrictive instability criteria. In the present example, perturbations with an out of plane extension of the dam are probably able to activate a significant proportion of the bifurcation domain. Such perturbations are likely to exist in practice since the plane strain condition is strictly valid only for a dam of infinite out of plane length. Out-of-plane extension might come for instance from displacements of the lateral supporting points or from the digging of a transverse trench in maintenance work or after overtoping erosion. A 3D FEM modeling of the dam should be considered to simulate such perturbations.

In the present study, an analytical expression of the second-order work criterion has been derived for the specific constitutive behavior of Eq. (2). However, it should be underlined that directional analyses can be performed numerically at the material point scale with any kind of rate-independent constitutive behavior. Among others, this include the use of micromechanical models [17] or even discrete element modeling (DEM) [19] in case FEMxDEM approaches are considered. A proof of feasibility has been performed in the present study (not shown here) and the analytical results of Eqs. (5) and (6) have been recovered with auxiliary FEM computations on a unit volume of material. Before conducting the directional analysis, this unit volume was pre-loaded according to the stress states encountered in the dam body.

Even if the present study highlights the potential use of the bifurcation domain concept at the scale of an engineering structure, there is now an inverse problem to solve to identify the adverse changes in the boundary conditions that will effectively trigger the underlying material instabilities. Eventually, we will need to assess whether the mode of control may allow the inertial transition to take place leading to the dam liquefaction. The answers to these questions are the last missing links to making an efficient use of the second-order work criterion in practical design of engineering structures.

References

1. Bigoni, D., Hueckel, T.: Uniqueness and localization—I. Associative and non-associative elastoplasticity. Int. J. Solids struct. 28(2):197–213 (1991)
2. Bishop, A.W.: The use of the slip circle in the stability analysis of slopes. Geotechnique **5**(1), 7–17 (1955)
3. Commissariat à l'Energie Atomique (CEA) - DEN/DM2S/SEMT. Cast3M finite element code. http://www-cast3m.cea.fr/ (2017)
4. Hill, R.: A general theory of uniqueness and stability in elastic-plastic solids. J. Mech. Phys. Solids **6**(3), 236–249 (1958)
5. Hu, J., Li, Z., Darve, F., Feng, J.: Advantages of second-order work as a rational safety factor and stability analysis of a reinforced rock slope. Can. Geotech. J. **57**(5), 661–672 (2020)
6. Laouafa, F., Prunier, F., Daouadji, A., Gali, H.A., Darve, F.: Stability in geomechanics, experimental and numerical analyses. Int. J. Numer. Anal. Methods Geomech. **35**(2), 112–139 (2011)
7. Lignon, S., Laouafa, F., Prunier, F., Khoa, H., Darve, F.: Hydro-mechanical modelling of landslides with a material instability criterion. Geotechnique **59**(6), 513–524 (2009)
8. Mandel, J.: Conditions de stabilité et postulat de drucker. In: Rheology and soil mechanics/Rhéologie et mécanique des sols, pp. 58–68. Springer (1966)
9. Mestat, P.: Lois de comportement des géomatériaux et modélisation par la méthode des éléments finis. Etudes et recherches des laboratoires des ponts et chaussées-série géotechnique (GT 52) (1993)

10. Nicot, F., Lerbet, J., Darve, F.: Second-order work criterion: from material point to boundary value problems. Acta Mechanica **228**(7), 2483–2498 (2017). https://doi.org/10.1007/s00707-017-1844-1
11. Nicot, F., Sibille, L., Darve, F.: Bifurcation in granular materials: an attempt for a unified framework. Int. J. Solids Struct. **46**(22–23), 3938–3947 (2009)
12. Prunier, F., Laouafa, F., Lignon, S., Darve, F.: Bifurcation modeling in geomaterials: from the second-order work criterion to spectral analyses. Int. J. Numer. Anal. Methods Geomech. **33**(9), 1169–1202 (2009)
13. Prunier, F., Nicot, F., Darve, F., Laouafa, F., Lignon, S.: Three-dimensional multiscale bifurcation analysis of granular media. J. Eng. Mech. **135**(6), 493–509 (2009)
14. Rudnicki, J.W., Rice, J.: Conditions for the localization of deformation in pressure-sensitive dilatant materials. J. Mech. Phys. Solids **23**(6), 371–394 (1975)
15. Sarma, S.: Seismic stability of earth dams and embankments. Geotechnique **25**(4), 743–761 (1975)
16. Spencer, E.: A method of analysis of the stability of embankments assuming parallel inter-slice forces. Geotechnique **17**(1), 11–26 (1967)
17. Veylon, G., Nicot, F., Zhu, H., Darve, F.: Microstructure incidence on the bifurcation domain topology in granular materials. J. Eng. Mech. **144**(6), 04018031 (2018)
18. Wan, R., Nicot, F., Darve, F.: Failure in geomaterials: a contemporary treatise. Elsevier (2017)
19. Wautier, A., Bonelli, S., Nicot, F.: Micro-inertia origin of instabilities in granular materials. Int. J. Numer. Anal. Methods Geomech. **42**(9), 1037–1056 (2018)
20. Xiong, H., Yin, Z.-Y., Nicot, F.: A multiscale work-analysis approach for geotechnical structures. Int. J. Numer. Anal. Methods Geomech. **43**(6), 1230–1250 (2019)
21. Zienkiewicz, O.C., Humpheson, C., Lewis, R.: Associated and non-associated visco-plasticity and plasticity in soil mechanics. Geotechnique **25**(4), 671–689 (1975)